

# Effect of Alkaline and Hot Water Treatments on the Structure and Morphology of Piassava Fibers

*Eduardo Braga Costa Santos<sup>b</sup>, Camila Gomes Moreno<sup>a</sup>, Janetty Jany Pereira Barros<sup>a</sup>, Danusa Araújo de Moura<sup>a</sup>, Fabiana de Carvalho Fim<sup>a</sup>, Andreas Ries<sup>c</sup>, Renate Maria Ramos Wellen<sup>a,b</sup>, Lucineide Balbino da Silva<sup>a,b\*</sup>*

<sup>a</sup>*Departamento de Engenharia de Materiais, Centro de Tecnologia, Universidade Federal da Paraíba, João Pessoa, PB, Brazil*

<sup>b</sup>*Programa de pós-graduação em Ciência e Engenharia de Materiais, Universidade Federal da Paraíba, João Pessoa, PB, Brazil*

<sup>c</sup>*Departamento de Engenharia Elétrica, Universidade Federal da Paraíba, João Pessoa, PB, Brazil*

Received: April 10, 2017; Revised: November 20, 2017; Accepted: December 14, 2017

The effect of alkaline and hot water surface treatments of piassava *Attalea funifera* fibers was investigated. The efficiency of each treatment was evaluated by Fourier transform infrared spectroscopy, X-ray diffractometry, optical microscopy, scanning electron microscopy and atomic force microscopy. The alkaline treatments were effective in removing the superficial lignin layer from the fiber, while the hot water treatment was not. Treatment with hot water and NaOH caused fiber defibrillation. NaOH was most effective in promoting both, a decrease in fiber diameter and an increase in fiber surface area. Treatment with  $\text{Ca}(\text{OH})_2$  led to the formation of a  $\text{CaCO}_3$  layer deposited on the fiber, preventing defibrillation. The crystalline structure of the fiber was not altered by any of the treatments, maintaining type I cellulose.

**Keywords:** *Piassava fibers, surface treatment, FTIR, BET, DRX.*

## 1. Introduction

Nowadays the research field of ecofriendly polymer composites has provided numerous studies on potential uses of various plant fibers (e.g. sisal, jute, linen, hemp, etc.) as filler materials with the ability to reinforce the polymer. The great interest in plant fibers is due to their classification as renewable sources, combined with low cost availability, low density, non-toxicity, recyclability; also such plant fibers are non-abrasive and do not damage the machines for processing the polymer composites<sup>1,2</sup>. Each fiber type has specific properties depending on the nature of the plant, the region where it has grown, the plant age and the extraction method used<sup>3</sup>. Therefore, many studies have been published with the aim to understand the structural and morphological characteristics of vegetable fibers subjected to various surface treatments. For instance, maceration with sodium hydroxide, acetylation, benzoilation, oxidative attack with peroxide and silane coupling are attempts to improve the interaction at the fiber-polymer interface in composites<sup>1,4,5</sup>.

The structure of the plant fibers consists of two distinguishable regions: crystalline cellulose and an amorphous region containing hemicellulose, lignin, pectin and greases. Among these constituents, cellulose is the most important part for assigning strength, stiffness and dimensional stability of the fibers due to its crystalline structure<sup>6</sup>. Furthermore, this constituent is a natural polymer consisting of linear

anhydrous D-glucose repeating units ( $\text{C}_6\text{H}_{11}\text{O}_5$ ) linked together by 1,4- $\beta$ -D-glycosidic bonds at C1 and C4 positions. The final cellulose structure is governed by both intramolecular and intermolecular hydrogen bonds, which maintain the structure of cohesive cellulose<sup>7</sup>.

Typically cellulose is biosynthesized in its metastable form, known as cellulose I, forming crystalline microfibrils with packaged macromolecular chains in parallel. Hemicellulose, unlike cellulose, comprises a group of polysaccharides consisting of a combination of sugars with rings of 5 and 6 carbon atoms, forming a variety of complex amorphous molecules, with units of D-xylose, D-glucose and D-glucuronic acid. These units are formed of carbon chains with a hydroxyl group except those forming carbonyl or hemiacetal bonds. Furthermore, hemicellulose is very hydrophilic and readily soluble in basic media, as well as hydrolyzed in acids<sup>8,9</sup>.

Contrary to this, lignin is a highly complex, aromatic and amorphous polymer, the generic building block are phenylpropane units; it has the lowest water absorption capability among other components of vegetable fibers<sup>10</sup>. The aromatic parts can be p-hydroxyphenyl, guaiacyl and syringyl units in different proportions, according to the origin of the fiber. Lignin is totally insoluble in most solvents, but it is soluble in hot bases<sup>8,10,11</sup>.

Considering the cell wall, the plant fiber consists of a primary layer S1 and another secondary layer S2. These walls are layers of cellulose microfibrils, consisting of a bundle of

\*e-mail: [lucineide@ct.ufpb.br](mailto:lucineide@ct.ufpb.br)

aggregated elementary cellulose fibrils; every fibril contains around 50 to 80 aligned cellulose molecules. The cellulose content in the fiber wall increases from wall S1 to wall S2, whereas the hemicellulose content is similar in S1 and S2. Lignin content reduces from wall S1 to S2.

Hemicellulose molecules are connected to cellulose fibrils through hydrogen bonds, also abundantly present between cellulose macromolecules in the fiber cell walls. However, these links may be broken when the fiber surface is in contact with atmospheric humidity; then the hydroxyl groups from hemicellulose form new hydrogen bonds with water molecules, turning the fiber hydrophilic. This weakens the interaction of the fibers with non-polar (hydrophobic) polymeric matrices, compromising the mechanical properties of the composites. Already lignin and pectin act as an adhesive in the fiber structure, keeping all the constituents of the fiber together, giving integrity and mechanical strength to the fibers<sup>3,12,13</sup>.

The maceration of vegetable fibers using sodium hydroxide has been studied extensively<sup>5,14-18</sup> in order to remove natural oils covering the outer surface of the cell wall fibers, as well as pectin, lignin and hemicellulose. The process also modifies the surface of the fiber in terms of increased roughness, breaking some microfibril bundles, leading to defibrillation and individualization of microfibrils<sup>3</sup>. Therefore, many literature studies report surface modifications with sodium hydroxide of jute fibers, sisal, hemp, flax<sup>3,15,19-20</sup>; however, few studies have been proposed for modifying the surface of fiber residues, a by-product from manufacturing processes of vegetal fibers<sup>21</sup>.

The main contribution of this study is to evaluate surface modifications of the piassava fibers, a by-product of the broom manufacturing in the Brazilian Northeast region, with the potential to act as reinforcement in polymer biocomposites.

Our motivation is based on results by others<sup>20-22</sup>, comparing the effects of surface modifications with alkali treatment and hot water. Some studies<sup>20-22</sup> claim that hot water treatment is less aggressive the fiber surface, it does not cause deterioration of the primary cell wall (S1), and only removes non-cellulosic components degrading at low temperature. Hot water treatments also do not generate toxic products that are harmful to the environment.

The aim of this study is to evaluate different surface modifications of piassava fiber caused by alkaline treatment with NaOH and Ca(OH)<sub>2</sub> as well as by hot water at 75°C. The changes in surface morphology were investigated using a set of complementary techniques such as infrared spectroscopy, X-ray diffraction, optical microscopy, electron microscopy, atomic force microscopy, BET surface area evaluation and the size determination of the fiber particles.

## 2. Experimental

### 2.1 Materials

Piassava fiber from the species *Attalea funifera martius* was kindly donated by the company "Bruxaxá Vassouras e utensílios", located in Recife-Brazil. Analytical grade calcium

hydroxide and sodium hydroxide were purchased from Synth (Brazil), and used without any further purification.

### 2.2 Surface Treatments

The fiber as received from the supplier, in this work denominated as "*in natura*", was cut into strips with length ranging from 1 to 5 cm. One part was milled, weighed and stored in a desiccator; the other part was washed with a 2% neutral detergent solution, oven dried at 70°C for 2h and ground in a Knife Mill. The fibers were then sieved using a sieve shaker consisting of a cascade of different meshes (50, 60, 80, 100, 200 and 270 mesh). The fiber particle size adopted in this study was less than 270 mesh.

#### 2.2.1 Treatment with hot water at 75°C

1g of the washed fiber was stirred in 47 ml distilled water for 2, 12 and 24 hours. Afterwards, the fiber was then air dried for 168 ± 2 hours, weighed and stored in a desiccator.

#### 2.2.2 Alkaline treatment

1.5g of washed fibers were suspended in 7ml of 2wt% NaOH or Ca(OH)<sub>2</sub> solution. For analysis of the processing time, samples were stirred for a time period varying between 50 and 400 min. After filtration, the wet samples were weighed every 25 min, resulting in fifteen measurements during the evaluated period of time. The samples were then air dried for 48 h, weighed and stored in a desiccator. The alkali concentration was also analyzed, and alkaline solutions were prepared with the concentration of 2, 4, 6 and 8wt% of NaOH and Ca(OH)<sub>2</sub> and applied for the predetermined time. The sample weight measurements were performed with wet samples after immersion into the solutions and after air drying for 48 hours.

### 2.3 Mass Gain and Mass Loss

The mass gain was calculated with the wet sample immediately after treatment, i.e. Wfw-Wi, where Wfw is the sample weight shortly after treatment and Wi is the initial weight of the washed sample without surface treatment (Wi). The mass loss was calculated as Wfd - Wi, where Wfd is the weight of the treated sample after air drying for 48h.

### 2.4 Moisture Content

The moisture absorption and reabsorption tests of the fiber "*in natura*" and the fibers submitted to surface treatments were carried out according to the ASTM D1348-94 standard (Moisture content in cellulose materials), where test method B was used. Calculation of the moisture content was obtained using the equation (1):

$$\text{moisture content (\%)} = \left[ \frac{(M - D)}{(M - T)} \right] \times 100 \quad (1)$$

where: M is the original mass of the sample with the weight of the container; D is the final dry mass of the sample with the container; T is the mass of the empty sample vessel.

## 2.5 Characterization

### 2.5.1 Microscopy Analysis

For **optical microscopy** analysis, around 1g of the fibers were compacted into a circular pellet form and examined in a Zeiss Optical Microscope, model AxioTech 30; images were captured by an attached camera (model ColorView, AnalySIS image capturing software). Images were recorded with magnification of 5x, 10x, 20x and 50x.

**Scanning Electron Microscopy (SEM)** analyses were performed on a Leo 1430 unit from Zeiss detecting secondary electrons. Samples were metalized with gold prior to analysis.

**Atomic Force Microscopy (AFM)**, analyses were performed on a Confocal Raman-AFM Microscope, model Alpha 300 AR, from WITEC. An aluminum cantilever ( $k = 0.2 \text{ N/m}$ ) was used; for every image, 256 points per line were obtained at a scanning speed of 1 s/line.

### 2.5.2 Surface Area and Particle Size

Fiber surface area analysis was performed in a Surface Area and Porosity Analyzer, model ASAP 2420, from Micromeritics. Initially the samples were treated for 4 hours at  $120^\circ\text{C}$  in a BelprepII from Bel Japan under nitrogen flow. The samples were then subjected to sorption in gaseous nitrogen, applying He standard in a dewar containing liquid nitrogen.

Particle size analyses of the samples were performed on a S3500 unit from Microtrac. All analyses were done three times by wet flow. The samples were immersed in ethanol-acetone mixture.

### 2.5.3 Fourier Transform Infrared Spectroscopy (FT-IR)

The fiber analyses were recorded on an IR-Prestige 21 spectrophotometer from Shimadzu Model accumulating 32 scans with  $4 \text{ cm}^{-1}$  resolution in the  $4000$  to  $400 \text{ cm}^{-1}$  region. Samples were prepared as KBr pellets (1 wt% fiber content).

### 2.5.4 X-ray diffraction (XRD)

X-ray diffraction patterns of the fibers were recorded on a D8 Advance Davinci unit from Bruker under the following conditions:  $\text{CuK}\alpha$  radiation, 40 kV and 40 mA anode current, Ni filter,  $0.6^\circ/\text{min}$  scanning speed.

The crystallinity index (ICr) of the fibers was evaluated from the XRD intensity data of the crystalline and amorphous fiber phase, determined using Segal's formula<sup>23</sup>:

$$ICr = 100 \times [(I_{002} - I_{am}) / I_{002}] \quad (2)$$

where:  $I_{002}$  is the intensity of the crystalline part of the cellulose fiber (i.e., for pure cellulose) and  $I_{am}$  is the intensity of the very broad peak of the amorphous contents (i.e., cellulose, hemicellulose and lignin); according to the literature these parts generate a peak at  $2\theta = 16^\circ$ <sup>11</sup>.

## 3. Results and discussion

### 3.1 Infrared analysis

Infrared analyses were performed for fibers "in natura" and fibers subjected to surface treatments. The conditions these treatments were determined based on the water absorption results of the treated fibers discussed in the following sessions. The infrared spectra of the fibers are shown in Figure 1, detecting the main functional groups of the components that constitute the piassava fiber. Table 1 shows the principal vibration modes as obtained from the spectra of Figure 1, together with their respective assignments to the fibers' components.

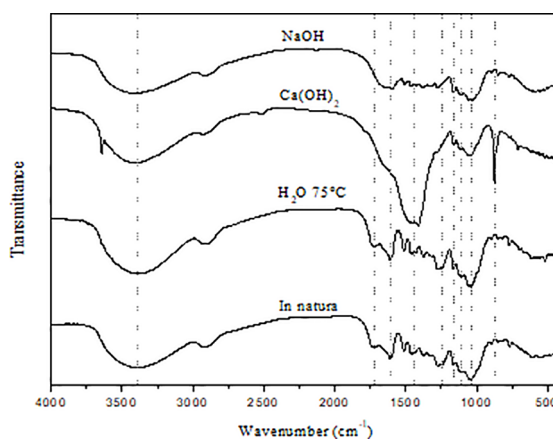


**Figure 1.** FTIR spectra of the piassava fiber "in natura" and after different surface treatments.

The spectra can be divided into two principal transmittance regions: first, the high wavenumber range from  $3750$  to  $2800 \text{ cm}^{-1}$ , then a second region with lower wavelengths, from  $1800$  to  $700 \text{ cm}^{-1}$ . The functional groups characteristic for cellulose appear at  $3340 \text{ cm}^{-1}$  referring to O-H stretching vibrations, due to hydrogen bonding in cellulose. According to Abidi et al<sup>24</sup>, this  $3340 \text{ cm}^{-1}$  vibration is attributed to intramolecular hydrogen bonding.

The vibrations at  $2930$  and  $2877 \text{ cm}^{-1}$  refer to stretching of aliphatic C-H bonds, here available in the form of methyl and methylene groups, respectively.

The bands at  $1270$ ,  $1168$  and  $1047 \text{ cm}^{-1}$  are attributed to stretching vibrations of the C-O-C group, present in the glucose rings<sup>1</sup> of cellulose. The vibration at  $898 \text{ cm}^{-1}$  is due to  $\beta$ -glycosidic binding<sup>24</sup>. Zhang et al.<sup>1</sup> called this  $898 \text{ cm}^{-1}$  band a characteristic feature of the crystalline phase of type I cellulose.

Regarding hemicellulose, the bands in  $3340$ ,  $2877$  and  $898 \text{ cm}^{-1}$  are equally attributed to the O-H, aliphatic C-H

**Table 1.** IR bands and their proposed associations to the infrared spectra of fiber components.  $\nu$  = stretching vibrations,  $\delta$ = deformation bands.

IR region (cm <sup>-1</sup> )	Absorption peak (cm <sup>-1</sup> )	Peak attribution	
3750-2800	3644	$\nu(\text{OH})$	
	3340	$\nu(\text{OH})$	
	2930	$\nu_a(\text{CH})_{\text{CH}_2}$	
	2877	$\nu_s(\text{CH})_{\text{CH}_2}$	
1800-1500	1724	$\nu(\text{C}=\text{O})$	
	1610	$\nu(\text{C}=\text{C})$	
	1513	$\nu(\text{CH})$	
1500-1100	1470	$\nu(\text{CO}_3)$	
	1453	$\delta(\text{CH}_3)$ , $\nu(\text{C}=\text{C})$	
	1423	$\nu(\text{O}-\text{CH}_3)$	
	1375	$\delta(\text{CH})$	
	1270	$\nu(\text{C}-\text{O}-\text{C})$	
	1246	$\nu(\text{C}-\text{O})$	
	1168	$\delta(\text{C}-\text{O}-\text{C})$	
	1112	$\nu(\text{C}-\text{O})$	
	1100-400	1047	$\nu(\text{C}-\text{O})$
		898	$\beta$ -glycosidic bonding
878		$\delta(\text{CO}_3)$	
823		$\nu(\text{C}-\text{H})$ aromatic	

and  $\beta$ -glycosidic binding. These characteristic bands are also present in hemicellulose. The presence of a vibration at 1724 cm<sup>-1</sup>, being characteristic for unconjugated carbonyl groups (C=O)<sup>25</sup>, is representative for hemicellulose, as well as a band at 1246 cm<sup>-1</sup>, which is associated to the acetyl group<sup>24</sup>.

The typical C-H and O-H stretching vibrations are also present in lignin. Besides that, lignin exhibits his own characteristic vibrations at 1610, 1453 and 823 cm<sup>-1</sup>, referring to its aromatic structure<sup>26</sup>. Another characteristic lignin band at 1423 cm<sup>-1</sup> is assigned to the -O-CH<sub>3</sub> stretching vibration in methoxy groups, while two bands at 1168 and 1112 cm<sup>-1</sup> refer to the C-O-C and C-O (in alcohols) group, respectively. According to Saliba et al.<sup>27</sup>, the C-O bonds, present in all three types of aromatic units that can form the lignin structure, exhibit some wavenumber variations in the IR spectrum (Figure 1).

In guaiacyl rings, the C-O band appears in the range from 1275 to 1265 cm<sup>-1</sup>, in syringe rings this range is shifted to 1240-1230 cm<sup>-1</sup> and the phenolic C-O vibrations exhibit shorter wavenumbers, close to 1200 cm<sup>-1</sup>. Therefore, the lignin present in the piassava fiber consists mostly of the aromatic guaiacila and syringil units.

Based on the results presented in Figure 1 and Table 1, it can be suggested that only the treatments with Ca(OH)<sub>2</sub> and NaOH were efficient regarding the total or partial removal of hemicellulose and lignin. This can be proved by the disappearance or loss of intensity of the main hemicellulose bands (1724 cm<sup>-1</sup>) and lignin bands (1423, 1270, 1246 and 823 cm<sup>-1</sup>). Due to the fact that the band at 1270 cm<sup>-1</sup> can

be associated to both, cellulose (glucose rings) and lignin (guaiacyl rings), it does not disappear completely but loses intensity, which can be attributed to the solubilization of Lignin; cellulose is still present in the fiber structure after all alkaline treatments.

The main difference between samples treated with calcium hydroxide and sodium hydroxide are the bands at 3644, 1470 and 878 cm<sup>-1</sup>, attributed to O-H stretching as well as to stretching and deformation of the carbonate (CO<sub>3</sub><sup>2-</sup>) anion. This narrow peak at 3664 cm<sup>-1</sup> is characteristic for a phase mixture, rather than a single phase of pure calcium hydroxide<sup>28</sup>.

The appearance of bands characteristic for carbonate indicates the formation and deposition of only little water soluble calcium carbonate at the surface of the fibers according to the following reaction<sup>29</sup>:



Both alkaline solutions (NaOH and Ca(OH)<sub>2</sub>) react with carbon dioxide from the air, but sodium carbonate is easily soluble in water and consequently not deposited on the surface of the fibers.

The deposition of some crystalline material on the surface of the fibers can be confirmed by SEM images (Figure 2c). Furthermore, the inset of this Figure (higher magnification) suggests a deposition of these crystals in pores and in the cracks of the fiber, thus causing a coating on the fiber. Besides that atomic force microscopy (Figure 3e) also supports the existence of a deposited calcium carbonate layer.

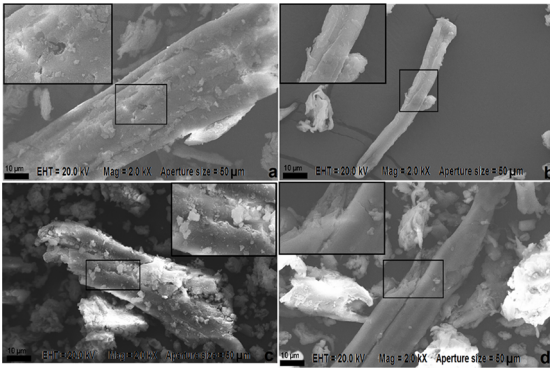


**Figure 2.** Scanning electron microscopy images of different fiber surfaces: a) "In natura", b) treated with NaOH, c) treated with  $\text{Ca}(\text{OH})_2$ , d) treated with hot water (75°C).

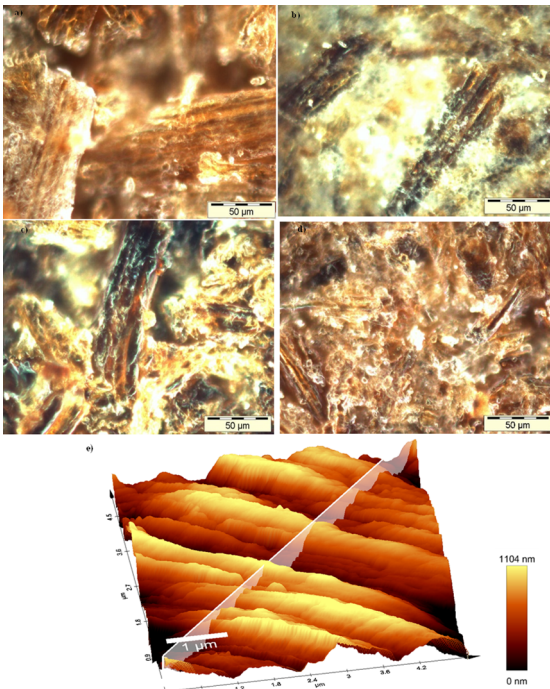


**Figure 3.** Optical microscopy images of fibers (magnification 50 times): a) "In natura", b)  $\text{Ca}(\text{OH})_2$ , c) NaOH, d) 75°C, e) Atomic force micrograph of the surface of a fiber treated with  $\text{Ca}(\text{OH})_2$ .

Comparing fibers "in natura" with those treated with hot water, the only difference is the intensity of the vibration bands. So this treatment can be considered efficient for the removal of greasy materials and dirt, as can be observed from the morphological aspect of this fiber in Figure 2d. Dirt and other greasy materials will hinder the adhesion of the fiber to any polymer matrix.

### 3.2 Microscopic Characterization

Within the analysis by Scanning Electron Microscopy, it is possible to verify the defibrillation process in the fibers submitted to treatment with NaOH and heat, as it can be observed in Figures 2b and d, respectively. The "in natura"

fiber is intact (Figure 2a), and the bundles of microfibrils are covered by the natural constituents that define the top of fiber (waxes, pectins, lignin). The treatment with NaOH (Figure 2b) was the best in increasing fiber surface steadiness and roughness (Figure 2b), also decreasing fiber diameters (Figure 2c) when comparing its topographic characteristics with the surrounding "in natura" fiber (Figure 2a). This effect confirms the findings of several authors<sup>5,17,30-32</sup>, who suggested that NaOH treatment brings about the rupture of bundles of microfibrils, producing defibrillation and individualization. These changes can potentially result in an increase in the effective area of the available fiber surface, improving the interfacial interaction in the fiber with the polymer matrices. Defibrillation also took place in the treated fiber with hot water, although the top of fiber is apparently smoother (Figure 2d), i.e., quite a bit less rough as the surface part of the NaOH treated fiber. Shown in Figure 2c, on the surface of the fiber treated with  $\text{Ca}(\text{OH})_2$ , the deposition of crystals can be observed, probably of calcium carbonate, as suggested by infrared analysis.

Morphological examinations were conducted to evaluate the surface topographic characteristics of the fibers and to understand the consequences of treatments on those surfaces better. In Figures 3a-d, the micrographs obtained by optical microscopy are shown. It may be observed the treatment of the "in natura" fiber with  $\text{Ca}(\text{OH})_2$  and NaOH at 2 wt.% for 225 minutes and 75°C water for 24 hours. The outer lining characteristics of the fibers are different from each other. The outer lining of the fiber "in natura" (Figure 3a) is shown to be intact, and the well-bonded microfibrils bundles may be observed, although they are not as clear than those seen in the fibers treated with the alkaline solution (Figure 3b-c). Nevertheless, in the micrograph of the  $\text{Ca}(\text{OH})_2$  treated fiber (Figure 3b), it can be observed a whitish region across the fiber, in accordance with the infrared analysis that shows the forming of calcium carbonate on top of the fiber. It was also feasible to observe a coating on top of the fiber that also colludes with this hypothesis by atomic force microscopy (AFM), as it may be seen in Figure 3e. In the fiber treated with NaOH, no whitish region was found, besides the white region created due to the light beam used to capture the image. An alternative morphological aspect was observed for the fiber submitted to the thermal treatment, and it seemed that the mixture with intact fiber and with microfibrils occurred as a result of defibrillation.

### 3.3 Surface Treatments

Within an alkaline treatment, the reaction time and the alkaline concentration are both the most critical reaction parameters in a fiber surface treatment. Thus, it was initially determined the optimal time for alkaline treatments on the basis of the weight gain of the treated fibers while wet, and on the weight reduction after drying. Figure 4a displays the weight gain curves of the moist specimens right after the



processing of the alkaline treatments. Between 50 and 75 minutes, a growth around 50% was observed in the weight gain of the samples. For both samples, after that increase, a reduction in the bulk gain can be observed. Shortly after, the weight gain returned, outstanding at a plateau from the 125th to the 175th minute, sustaining at virtually the exact same value of weight gain seen at 75 minutes. From a previous FTIR examination, it was remarked that, at 225 minutes, the alkaline treatments led to removing the light ingredients (lignin, hemicellulose), concurring with the observed effect at the 225th minute, by which the weight loss of the samples occurred. Lignin is in charge of the lower water assimilation of the fiber<sup>10</sup>. Therefore, its removal increased the permeability of the fiber, and from 250 minutes onwards, the fiber regained weight. The sample handled with NaOH exhibited larger weight gain with time than the sample handled with  $\text{Ca}(\text{OH})_2$ . Based on these results, two assumptions can be devised. First, treatment with calcium hydroxide was demonstrated to be less aggressive to the surface of the fiber than the NaOH treatment. Secondly, the larger weight gain of the NaOH handled fiber indicates that a larger amount of water penetrated its structure, consequently defibrillating the fiber and reducing its size (as seen in Figure 3b), as the fiber handled with  $\text{Ca}(\text{OH})_2$  did not defibrillate (as seen in Figure 3c). As proposed by FTIR and seen in Figure 2e, the calcium carbonate development could have stopped the defibrillation of the fiber undergoing that treatment.

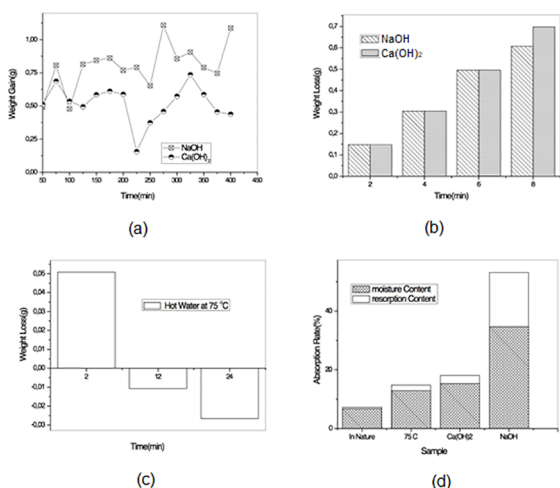


**Figure 4.** a) Fiber Mass Gain according to time after alkaline treatments at 2 wt.%; b) Mass loss according to the concentration of NaOH and  $\text{Ca}(\text{OH})_2$ ; c) Mass loss according to treatment time with hot water at 75°C, varying the treatment time in 2, 12 and 24 hours, and d) Moisture absorption and reabsorption rate of the "in natura" fiber treated with hot water, NaOH and  $\text{Ca}(\text{OH})_2$ .

For both alkalis, the procedure time of 225 minutes was used to estimate the influence of their concentrations on the superficial treatment of the fiber, since it was at that time that the fiber lost less weight. Considering that a severe weight loss of the fiber could lead to its embrittlement<sup>33</sup>, that situation

is not of interest regarding its performance as a support in polymer composites. Many authors<sup>3,5,6,14-18</sup> observed that solutions with alkaline contents below 8% were the most found in the treatments, mainly around 4 to 5% of NaOH for removing lignin and hemicellulose from the surface of the fiber. Consequently, the concentrations studied were 2, 4, 6 and 8 wt.% of NaOH and  $\text{Ca}(\text{OH})_2$ . The weight loss data after the surface treatments and sample drying are shown in Figure 4b. It can be recognized that the increase of alkali concentrations also decreases the fiber mass. Accordingly, the removal of lignin and hemicellulose from the piassava fiber surface (used in this study as industrial waste) were observed, even at low concentrations of 2 wt.% of both alkalis.

In Figure 4c, it may be observed the influence of treatment time with hot water at 75°C on fiber weight loss, varying at 2h, 12h and 24h. It could be observed that, at 24h, the procedure triggered greater weight loss, with a mass decrease of approximately 17.72%, in accordance with the washed fiber before the surface treatment. According to SEM analysis, this result might be due to the removal of surface constituents of the treated fiber, by which an extremely clean surface may be observed with this fiber (Figure 3d). Removing the surface constituents may contribute to the interfacial interaction between fiber and polymer<sup>3</sup> in the case of using these fibers as filler in the preparation of polymer composites, considering that the cellulose OH-groups of the fibers may become more exposed to interact with the polymer<sup>33</sup>.

In Figure 4d, the absorption and moisture reabsorption data belonging to the fibers obtained from equation 1 can be observed. The reabsorption data reflect the ability of the totally dry fiber to reabsorb moisture, exhibiting the similar tendency observed for the absorption of humidity. It is noted that the "in natura" fiber and the fiber treated with hot water were the ones that presented lower absorption and reabsorption rates of moisture, while the fiber treated with NaOH was the one with higher values. The perceived range of moisture content data for "in natura" fibers and those treated with water at 75°C act accordingly with expected values for fibers<sup>12</sup>. According to Spinacé et al.<sup>10</sup>, lignin generates the lowest water absorption among the various other aspects of a vegetal fiber. While appraising the infrared spectrum in Figure 1, the presence of lignin can be observed in both, the "in natura" fiber and the thermally treated fiber. Consequently, lignin acts as an impermeable sheet for the penetration of moisture in the "in natura" fiber and the thermally processed fiber at 75°C. On the other hand, for fibers treated with NaOH and  $\text{Ca}(\text{OH})_2$ , the lignin and hemicellulose peaks were not observed, and this is especially true for any fiber treated with NaOH. Hence, removing surface components with alkali allowed the fiber to soak up an even larger volume of moisture on account of the exposure of OH groups belonging to the cellulose, making the alkali treated fiber more hydrophilic<sup>25</sup>.

Therefore, it can also be concluded that the NaOH treatment induced the fiber to soak up more moisture, creating

a more distended structure than obtained with  $\text{Ca}(\text{OH})_2$ , in agreement with the hypothesis that  $\text{Ca}(\text{OH})_2$  was less aggressive compared to  $\text{NaOH}$ .

### 3.4 Surface Area Characterization

In this study different surface treatments (with hot and alkaline water) were carried out with piassava fibers in order to obtain fibers with a cleaner surface and also to expose the hydroxyl groups that are present in the cellulose, composing the fiber. According to Li et al.<sup>33</sup>, any alkaline treatment of fiber, (sodium hydroxide most commonly used), can remove lignin and greases covering the outer surface of the cellular wall of the fiber, besides being able to promote the depolymerization of the cellulose. By the nitrogen adsorption analysis, it was possible to verify the influence of the different surface treatments on the texture properties of the piassava fiber. Table 2 shows the specific surface area data by BET method, the parameter C and the average pore diameter obtained by the BJH method.

**Table 2.** Properties of fibers after different treatments.

Fiber	$S_{\text{BET}}^1$ (m <sup>2</sup> /g)	$D_{\text{P(BJH)}}^2$ (Å)	Parameter C
In natura	58,20 ± 1,04	58,18	3,23
Water at 75 °C	52,82 ± 2,61	55,69	2,04
Treated with $\text{Ca}(\text{OH})_2$	66,70 ± 2,06	58,18	4,71
Treated with $\text{NaOH}$	173,71 ± 1,94	47,09	2,47

<sup>1</sup> $S_{\text{BET}}$  = surface area via BET method;

<sup>2</sup> $D_{\text{P(BJH)}}$  = mean pore diameter via BJH method.

The specific area results showed that the most water soluble base ( $\text{NaOH}$ ) promotes a greater increase in the surface area when compared to the surface area of the "in natura" fiber. This treatment was more efficient in a fiber cleaning process, removing greases and lignin, as evidenced by FTIR analysis.

According to the literature<sup>33,34</sup>, alkali may also promote the conversion of the hydroxyl groups present in cellulose to alkoxide, leading to fiber defibrillation. The increase in the surface area of the fiber treated with calcium hydroxide may indicate that some morphological change occurred in the fibers, however, the pore size remained the same as found for fibers "in natura".

It is interesting to mention that the reason for the non-decrease in pore size is due to the mineralization of the fiber surface, as can be visualized in the SEM analysis shown in Figure 3e. Therefore, we can suggest that a cleaning occurred on the surface of the fibers, resulting in pore exposure, however, these were covered with calcium carbonate (Figure 3c), since calcium hydroxide is poorly soluble in water and forms calcium carbonate when in contact with  $\text{CO}_2$  from the air, as already mentioned in the FTIR analysis.

In relation to the treatment with hot water we obtained a contradictory result, since there was a decrease in the surface area and also a decrease in the pore size in relation to fibers "in natura". However, the SEM analysis showed that defibrillation of the thermally treated fibers occurred with reduction of the fiber diameter (Figure 3d). Mulinari et al.<sup>21</sup> also observed that the fibers from the textile residue were modified through a heat treatment at 100°C, acquiring flattened forms. In addition, all the fibers presented pore size consistent with mesopore classification<sup>35</sup>.

The parameter C (BET method) is related to the enthalpy differences of the first and following layer of adsorbed nitrogen. Kádár et al.<sup>36</sup> proved that parameter C is strongly related to the surface energy of the fillers. From Table 2 can be seen that the parameter C is very similar for all samples, because it is the same fiber. What changes is the way the particles are aggregated to the surface after the chemical treatments. Extremely low parameter C values indicate very weak interactions between the nitrogen being adsorbed and the particles present on the surface of the fibers. The fiber treated with calcium hydroxide showed the highest value for parameter C, indicating that this procedure increases the fiber surface energy. This is due to the fact that calcium hydroxide, in contact with water, mineralizes and forms a layer that is more strongly bound to the surface and probably leaves a certain amount of OH groups available. The thermally treated fibers showed the lowest value of the parameter C, which leads us to assume that this treatment decreases the amount of OH groups available on the surface of the fibers, reducing its surface energy.

All adsorption and desorption isotherms of  $\text{N}_2$  for piassava fibers present a small hysteresis loop, characteristic for type IV isotherms, according to IUPAC (International Union of Pure and Applied Chemistry) classification (results not shown). This is typically attributed to mesoporous materials. The greater the dispersion of pore sizes, the more pronounced are the hysteresis. Furthermore, the shape of the hysteresis loop is H3 type, which is characteristic for aggregated plate-like particles giving rise to slit-shaped pores<sup>35</sup>.

These results corroborate the SEM images, which show the clear presence of slit-shaped pores in all fibers, as can be seen in the micrographs of Figure 3. Flat pores are formed when a part of the solid is removed, either by a process of partial solubilization of this solid, through reactions with formation and permeation of gases or, by separation of phases<sup>37</sup>. For all analyzed isotherms the adsorption volume increases with increasing relative pressure. This is an indication of a porous material with satisfactory adsorption properties<sup>1</sup>.

### 3.5 Characterization of Fiber Particle Size

The diameter distribution curves of the fibers are given in Figure 5, the values of the particle diameters are shown in Table 3. By assuming that the shape of the fiber diameter is cylindrical, it can be seen that all fibers have a Gaussian

frequency distribution. It can be seen in Figure 5 that fibers "in natura" and  $\text{Ca}(\text{OH})_2$  treated fibers present narrower particle size distributions than NaOH and hot water treated fibers. This means that the latter samples present a greater size variation. This result is supported by the morphological analysis; some images are shown in Figure 3. Both fibers, "in natura" and those treated with  $\text{Ca}(\text{OH})_2$ , did not show any indication that fibrillation occurred.

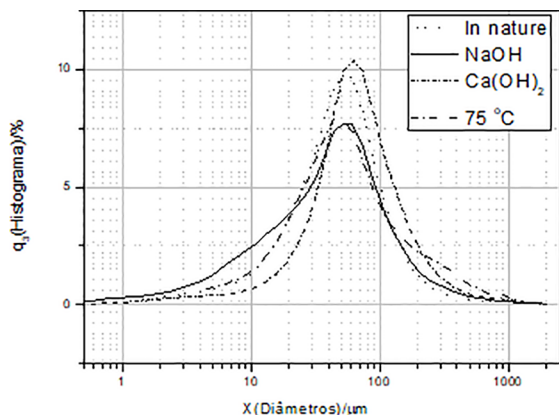


**Figure 5.** Particle size of the fibers: "In natura", treated with  $\text{Ca}(\text{OH})_2$ , NaOH and with hot water at 75°C.

**Table 3.** Fiber diameters.

FIBER	$\bar{D}_V(\mu\text{m})$	$\bar{D}_N(\mu\text{m})$	$\bar{D}_A(\mu\text{m})$	SA
In natura	62.88	0.978	19.16	$3.13 \times 10^{-1}$
Treated with water at 75 °C	87.66	0.797	16.00	$3.75 \times 10^{-1}$
Treated with 2% $\text{Ca}(\text{OH})_2$	87.68	1.149	26.57	$2.26 \times 10^{-1}$
Treated with 2% NaOH	63.85	0.681	12.32	$4.87 \times 10^{-1}$

$\bar{D}_V$  = average diameter, in  $\mu\text{m}$ , volume distribution;

$\bar{D}_N$  = average diameter, in  $\mu\text{m}$ , number distribution;

$\bar{D}_A$  = average diameter, in  $\mu\text{m}$ , area distribution;

SA = specific surface area,  $\text{m}^2/\text{mL}$

On the other hand, defibrillation occurred in the fibers treated with NaOH and in those treated with hot water; the alkaline treatment was more effective for this purpose than hot water. The assumption of greater defibrillation of the NaOH-treated fibers is confirmed by observing smaller particle diameters, in the range of 0.6 to 11 microns that may be representative for microfibrils that have detached from these fibers. The fibers treated at 75°C also presented values in this range, but in a lower percentage, together with diameter values in the range of 100 to 1000 microns, which may reflect the presence of both fibrils and intact fibers.

An evaluation of particle diameters, shown in Table 3, points to lower values for the fibers treated with NaOH, followed by fibers treated with hot water. The highest specific surface area is in agreement with the result obtained by the

**Table 4.** Crystallinity index of piassava fibers "in natura" and after surface treatments.

Sample	Crystallinity index (%)
In Natura	30
Hot water 75 °C	32
Treated with 2%NaOH	44
Treated with 2% $\text{Ca}(\text{OH})_2$	23

BET method in Table 3 for this fiber. All these results are in good agreement with the morphological and FTIR results, which showed that there was a reduction in the diameter of the fiber, mainly due to treatment with NaOH leading to the removal of fiber extracts (wax, lignin and hemicellulose), respectively.

### 3.6 Structural Characterization of Fibers

The process of maceration of vegetable fibers using sodium hydroxide, depending on its concentration, may result in a polymorphic modification in the crystalline structure of the cellulose-I fibers, converting them to cellulose-II. That modification is due to a change in orientation of the cellulose crystalline chains, which in type I are parallel to each other, whereas in type II, the chains are aligned anti-parallel, which makes the structure of the fiber more voluminous, compared to cellulose-I<sup>38-39</sup>.

In the scientific literature, XRD data of fibers with cellulose-I structure are reported as 101, 101 and 002 planes, with peaks  $2\theta$  around the values 14°, 16° and 23°, respectively. The structure of cellulose-II presents an increase in intensity of the plane 021, at  $2\theta=20^\circ$ <sup>38-40</sup>. Ouajai et al.<sup>4</sup> studied the modification of flax fiber, varying the NaOH concentrations at 3, 5, 8, 10, 12, 15 and 20%. They observed that with increasing alkaline concentration, the crystalline transformation to cellulose-II caused a decrease in the intensity associated to the plane 002 and an increase in the intensity associated to the planes 101 and 021.

Figure 6 shows the XRD diffractograms of piassava fiber "in natura", treated with water at 75°C and with sodium and calcium hydroxide. It can be observed that the crystalline structure of the cellulose "in natura" and after both treatments is type I with angles  $2\theta$  around 16 and 22°. The pattern of the  $\text{Ca}(\text{OH})_2$  treated fibers show both, the characteristic pattern of cellulose and that of calcium carbonate deposited on the fiber surface (peak around  $2\theta=30^\circ$ )<sup>39</sup>.

None of the evaluated surface treatments altered the fiber crystal structure. As can be seen in Figure 6, the diffraction patterns are typical for cellulose I. Table 4 shows the crystallinity index data of the samples as calculated from equation 2. It can be observed that alkaline treatments with NaOH and with hot water at 75°C increased the crystallinity index of the piassava fibers, while the treatment with  $\text{Ca}(\text{OH})_2$  resulted in a decrease in that value, which is reflected in the decrease in intensity of the peak at  $2\theta=23^\circ$ . This decrease



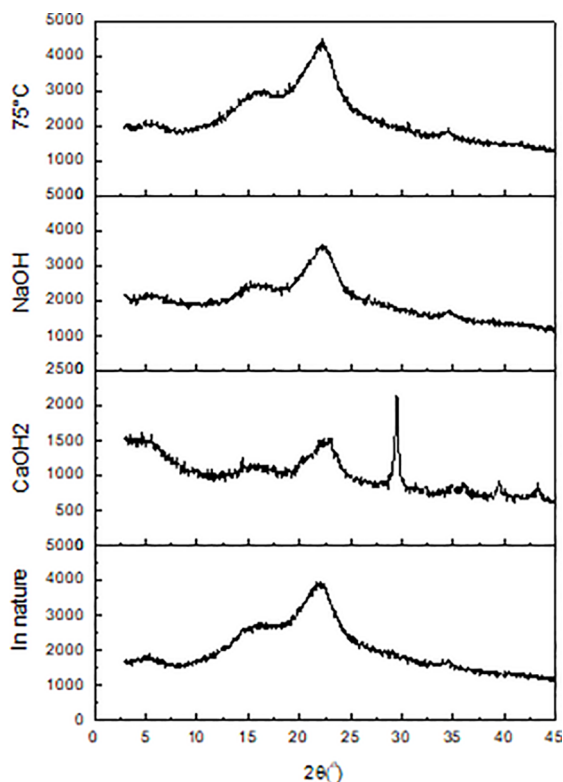


**Figure 6.** XRD diffractograms of piassava fibers: "In natura", treated with  $\text{Ca}(\text{OH})_2$ , NaOH and with hot water at  $75^\circ\text{C}$ .

in the intensity of the cellulose peak was also reported by Benitez-Guerrero et al.<sup>22</sup> when treating sisal fibers with calcium oxalate, attributing this decrease to the decomposition of the crystalline structure of cellulose. It can also be observed in the diffractograms that alkaline treatments of the fiber resulted in a decrease in the amorphous phase of the fiber, since a decrease in the intensity of the peak at  $2\theta=16^\circ$ , agrees with the infrared results, showing lignin removal from the surfaces of these fibers.

In the case of fiber treated with hot water at  $75^\circ\text{C}$ , an increase in the intensity of the cellulose peak can be observed, as its crystallinity index was the second highest when compared to the untreated ("in natura") fibers. This result is in agreement with those obtained by Mulinari et al.<sup>21</sup> who also observed that fibers from textile residues treated thermally at  $100^\circ\text{C}$  were more crystalline than untreated fibers.

#### 4. Conclusion

All the treatments studied did not alter the crystal structure of the fiber (type I cellulose). However, the treatment with sodium hydroxide resulted in a fiber with higher crystallinity index due to the removal of the non-cellulosic constituents. Alkaline treatments were effective in removing lignin from the fiber. Nevertheless, there are  $\text{Ca}(\text{OH})_2$  crystals remaining present on the surface of the fiber, which were not solubilized during treatment. The water

absorption results revealed the existence of an optimum time of the alkaline treatments equal to 225 min. After this processing time the fiber structure absorbed more water due to even more intense lignin removal. The treatment of the fiber with hot water did not show lignin removal from the fiber, but impurities were effectively removed from the fiber surface during 24 hours. The moisture absorption was more significant for the NaOH treated fiber due to the removal of the lignin layer, which is a quite impermeable layer of the fiber. Moreover, this alkali increased the surface area of the fiber, with an increase in approximately 198% with respect to "in natura" fiber. The porosimetry analysis via adsorption of  $\text{N}_2$  indicated the formation of slit-like mesopores in the surface of the fiber, particularly after the surface treatments. The particle size distribution was narrower for "in natura" fiber and  $\text{Ca}(\text{OH})_2$  treated fiber, being broader for the remaining treatments. Particle sizes in the range from 0.6 to 11 microns (representative for microfibrils) and from 100 to 1000 microns reflect the presence of both fibrils and intact fibers. Therefore, these latter treatments modified the surfaces of the piassava fiber, with topographic evidence, which allows to conclude that these treated fibers have the potential to be used in polymer composites.

#### 5. Acknowledgment

The authors thank FACEPE for financial support, CETENE for technical support, Capes for Eduardo Braga's scholarship, LSR and Lacom laboratories for the realization of morphological and FTIR characterizations.

#### 6. References

- Zhang T, Guo M, Cheng L, Li X. Investigations on the structure and properties of palm leaf sheath fiber. *Cellulose*. 2015;22(2):1039-1051.
- Oujai S, Hodzic A, Shanks RA. Morphological and grafting modification of natural cellulose fibers. *Journal of Applied Polymer Science*. 2004;94(6):2456-2465.
- Mwaikambo LY, Ansell MP. The effect of chemical treatment on the properties of hemp, sisal, jute and kapok fibres for composite reinforcement. *Macromolecular Materials and Engineering*. 1999;272(1):108-116.
- Oujai S, Shanks RA. Preparation, structure and mechanical properties of all-hemp cellulose biocomposites. *Composites Science and Technology*. 2009;69(13):2119-2126.
- Gutiérrez MC, De Paoli MA, Felisberti MI. Biocomposites based on cellulose acetate and short curauá fibers: Effect of plasticizers and chemical treatments of the fibers. *Composites Part A: Applied Science and Manufacturing*. 2012;43(8):1338-1346.
- Kabir MM, Wang H, Lau KT, Cardona F. Chemical treatments on plant-based natural fibre reinforced polymer composites: An overview. *Composites Part B: Engineering*. 2012;43(7):2883-2892.

7. Meyers MA, Chen PY, Lin AYM, Seki Y. Biological materials: Structure and mechanical properties. *Progress in Materials Science*. 2008;53(1):1-206.
8. John MJ, Thomas S. Biofibres and biocomposites. *Carbohydrate Polymers*. 2008;71(3):343-364.
9. Wang K, Yang HY, Feng X, Sun RC. Structural comparison and enhanced enzymatic hydrolysis of the cellulosic preparation from *Populus tomentosa* Carr., by different cellulose-soluble solvent systems. *Bioresource Technology*. 2011;102(6):4524-4529.
10. Spinacé MAS, Lambert CS, Femoselli KKG, de Paoli MA. Characterization of lignocellulosic curaua fibres. *Carbohydrate Polymers*. 2009;7(1):47-53.
11. Kumar R, Mago G, Balan V, Wyman CE. Physical and chemical characterizations of corn stover and poplar solids resulting from leading pretreatment technologies. *Bioresource Technology*. 2009;100(17):3948-3962.
12. Saheb DN, Jog JP. Natural fiber polymer composites: A review. *Advances in Polymer Technology*. 1999;18(4):351-363.
13. Taj S, Munawar MA, Khan SU. Natural fiber - reinforced polymer composites. *Proceedings of the Pakistan Academy of Sciences*. 2007;44(2):129-144.
14. Vilaseca F, Mendez JA, Pèlach A, Llop M, Cañigueral N, Gironès J, et al. Composite materials derived from biodegradable starch polymer and jute strands. *Process Biochemistry*. 2007;42(3):329-334.
15. Hossain MK, Dewan MW, Hosur M, Jeelani S. Mechanical performances of surface modified jute fiber reinforced biopol nanophased green composites. *Composites Part B: Engineering*. 2011;42(6):1701-1707.
16. Phuong NT, Solloguob C, Guinault A. Relationship between fiber chemical treatment and properties of recycled pp/bamboo fiber composites. *Journal of Reinforced Plastics and Composites*. 2010;29(21):3244-3256.
17. Ibrahim NA, Hadithon KA, Abdan K. Effect of Fiber Treatment on Mechanical Properties of Kenaf Fiber-Ecoflex Composites. *Journal of Reinforced Plastics and Composites*. 2010;29(14):2192-2198.
18. Ray D, Sarkar BK, Rana AK, Bose NR. Effect of alkali treated jute fibres on composite properties. *Bulletin of Materials Science*. 2001;24(2):129-135.
19. Dangtungee R, Tengsuthiwat J, Boonyasopon P, Siengchin S. Sisal natural fiber/clay-reinforced poly(hydroxybutyrate-cohydroxyvalerate) hybrid composites. *Journal of Thermoplastic Composite Materials*. 2015;28(6):879-895.
20. Le Duigou A, Bourmaud A, Balnois E, Davies P, Baley C. Improving the interfacial properties between flax fibres and PLLA by a water fibre treatment and drying cycle. *Industrial Crops and Products*. 2012;39:31-39.
21. Mulinari DR, Voorwald HJC, Cioffi MOH, Lima CAA, Baptista CAPR, Rocha GJM. Composite materials obtained from textile fiber residue. *Journal of Composite Materials*. 2011;45(5):543-547.
22. Benítez-Guerrero M, López-Beceiro J, Sánchez-Jiménez PE, Pascual-Cosp J. Comparison of thermal behavior of natural and hot-washed sisal fibers based on their main components: Cellulose, xylan and lignin. TG-FTIR analysis of volatile products. *Thermochimica Acta*. 2014;581:70-86.
23. Segal L, Creely JJ, Martin AE Jr., Conrad CM. An Empirical Method for Estimating the Degree of Crystallinity of Native Cellulose Using the X-Ray Diffractometer. *Textile Research Journal*. 1959;29(10):786-794.
24. Abidi N, Cabrales L, Haigler CH. Changes in the cell wall and cellulose content of developing cotton fibers investigated by FTIR spectroscopy. *Carbohydrate Polymers*. 2014;100:9-16.
25. Mortazavi SM, Moghaddam MK. An analysis of structure and properties of a natural cellulosic fiber (Leafiran). *Fibers and Polymers*. 2010;11(6):877-882.
26. Yang H, Yan R, Chen H, Lee DH, Zheng C. Characteristics of hemicellulose, cellulose and lignin pyrolysis. *Fuel*. 2007;86(12-13):1781-1788.
27. Saliba EOS, Rodriguez NM, Morais SAL, Piló-Veloso D. Lignins - isolation methods and chemical characterization. *Ciência Rural*. 2001;31(5):917-928.
28. Samanta A, Chanda DK, Das PS, Ghosh J, Mukhopadhyay AK, Dey A. Synthesis of Nano Calcium Hydroxide in Aqueous Medium. *Journal of the American Ceramic Society*. 2016;99(3):787-795.
29. Rodriguez-Navarro C, Suzuki A, Ruiz-Agudo E. Alcohol Dispersions of Calcium Hydroxide Nanoparticles for Stone Conservation. *Langmuir*. 2013;29(36):11457-11470.
30. Van de Weyenberg I, Truong TC, Vangrimde B, Verpoest I. Improving the properties of UD flax fiber reinforced composites by applying an alkaline fiber treatment. *Composites Part A: Applied Science and Manufacturing*. 2006;37(9):1368-1376.
31. Jähn A, Schröder MW, Fütting M, Schenzel K, Diepenbrock W. Characterization of alkali treated flax fibres by means of FT Raman spectroscopy and environmental scanning electron microscopy. *Spectrochimica Acta Part A: Molecular and Biomolecular Spectroscopy*. 2002;58(10):2271-2279.
32. Joseph PV, Joseph K, Thomas S, Pillai CKS, Prasad VS, Groeninckx G, et al. The thermal and crystallisation studies of short sisal fibre reinforced polypropylene composites. *Composites Part A: Applied Science and Manufacturing*. 2003;34(3):253-266.
33. Li X, Tabil LG, Panigrahi S. Chemical Treatments of Natural Fiber for Use in Natural Fiber-Reinforced Composites: A Review. *Journal of Polymers and the Environment*. 2007;15(1):25-33.
34. Mohanty AK, Misra M, Drzal LT. Surface modifications of natural fibers and performance of the resulting biocomposites: An overview. *Composite Interfaces*. 2001;8(5):313-343.
35. Sing KSW, Everett DH, Haul RAW, Moscou L, Pierotti RA, Rouquérol J, et al. Reporting Physisorption Data for Gas/Solid Systems with Special Reference to the Determination of Surface Area and Porosity. *Pure & Applied Chemistry*. 1985;57(4):603-619.
36. Kádár F, Százdi L, Fekete E, Pukánszky B. Surface Characteristics of Layered Silicates: Influence on the Properties of Clay/Polymer Nanocomposites. *Langmuir*. 2006;22(18):7848-7854.
37. Gregg SJ, Sing KSW. *Adsorption, Surface Area and Porosity*. London: Academic Press; 1982.

38. Qin C, Soykeabkaew N, Xiuyuan N, Peijs T. The effect of fibre volume fraction and mercerization on the properties of all-cellulose composites. *Carbohydrate Polymers*. 2008;71(3):458-467.
39. Krässig H. Structure investigations on cellulose fibers using infrared spectroscopy and x-ray diffraction. In: *Proceedings of the Eighth Cellulose Conference*; 1975 May 19-23; Syracuse, NY, USA. New York: John Wiley & Sons; 1976. p. 777-790.
40. Aydin M, Tozlu H, Kemalolu S, Aytac A, Ozkoc G. Effects of Alkali Treatment on the Properties of Short Flax Fiber-Poly(Lactic Acid) Eco-Composites. *Journal of Polymers and the Environment*. 2011;19(1):11-17.